



## A Wide-Range-Gain Switched-Coupled-Inductor Buck-Boost ZETA Converter

Mustafa Okati<sup>1</sup>, Mahdiyeh Eslami \*<sup>1</sup>, Mehdi Jafari Shahbazadeh <sup>1</sup>

<sup>1</sup>Department of Electrical Engineering, Kerman Branch, Islamic Azad University, Kerman, Iran.

Received: 01-Feb-2021, Revised: 31-Aug-2021, Accepted: 03-May-2021.

### Abstract

In the present work, an improved buck-boost converter with the possibility of flexible design is introduced to gain required voltage and easily adapt to any wide-range-gain application. Switched-coupled-inductors are employed as the key in this converter to achieve the wide-range-gain buck-boost operation through adjusting their turn ratio. The set of coupled-inductors are integrated with the conventional ZETA converter to be used in place of buck-boost cell of its original circuit, which relies on ZETA converter. This converter increased the voltage gain degree of freedom to design a wide-range gain operation for any required application. In comparison with the conventional competitors, the proposed converter is required to use smaller passive components with lower voltage and current ratings for its semiconductors. All these features and claims are investigated theoretically and then, are evaluated experimentally by implementing a test rig with the rated power of 200W.

**Keywords:** ZETA Converter, Switched-Coupled-Inductor, Wide-Range-Gain, Buck-Boost Converter.

### 1. INTRODUCTION

The renewable energy sources including the photovoltaic and the fuel cells have been widely employed recently for many industrial and domestic applications in order to provide cost-beneficial electrical energy. Each of

these sources generate the electricity with different properties of voltage and current, which may seriously restrict their applicability. For instance, their integration to the grid requires increasing their voltage to control the energy flow to the grid, while employing them as the energy source of some of home appliances need to decrease their voltage to avoid any damage due to

---

\*Corresponding Authors Email:  
mahdiyeh\_eslami@yahoo.com

overvoltage [1]–[6]. Therefore, in order to exploit their benefits out, a buck-boost converter is required to be employed as an interface between the end user and them to regulate the required voltage level. Literature presents many buck-boost DC-DC converters. Most of them are based on the conventional DC/DC converters including the buck, the boost, the buck-boost, the SEPIC, the CUK and the ZETA converters [7], shown in Fig.1. Analysis of ZETA converter in CCM (continuous conduction mode) was used in [8]. The main feature of the ZETA is converter isolated structure which allows tuning output voltage with only one power processing stage. The integration of conventional converters with the step-up/down techniques and circuits has resulted in a breed of buck-boost converters. The switched-capacitors/inductors [9]–[11], the voltage multiplier cells [12], [13], and their integrations are the most common techniques used in recently proposed converters. The converters in [14] and [15], a switched-capacitor/inductors is employed within the conventional buck-boost converter, which both offer quadratic voltage gain while suffering from a negative output voltage.

In [16]–[18], the presented converters are designed on the basis of the integration of the switched-capacitors/inductors and the multiplier cells to provide the buck-boost DC/DC converter. Numerous components are required by these converters, which incurs high cost of implementation. An extended multi cell buck-boost converter in terms of the conventional SEPIC converter is also provided in [19]. The same as previous converters, the one proposed in [19] needs a high number of components while the voltage gain is limited.

One of the well-known conventional DC-DC converters is the ZETA converter, which offers the buck-boost capability with the minimum number of components and thus the simplicity of implementation and operation. As the main drawback of the conventional ZETA converter, the limited voltage gain range withdraws its usage for the aforementioned applications. This leads to some modified and improved proposals compared to the conventional solutions. The converter in [20] is one of the recently proposed converters, which successfully employs an energy storing cell of switched-capacitors/inductor within the conventional

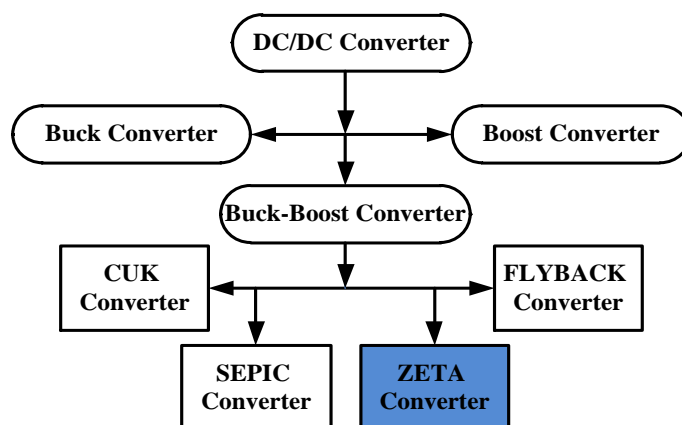


*Fig.1. Diversity of DC-DC Converters.*

ZETA converter. This converter offers a voltage gain only twice as that of the conventional ZETA converter while requiring a high number of components compared to its origin. This feature of its voltage gain restricts its superiority for the applications, where a wide-range-gain, especially the step-down operation, is required. In addition, the components' size may be still large such that degrades its usefulness for the applications, where the converter volume and cost are of concern.

Recently, the coupled-inductors are receiving more attention in the literature to be employed for improving the operation capabilities of any power converter and at the same time reducing the volume and the cost of its implementation. As an example, the converters proposed in [21]–[24] successfully employ the coupled-inductors integrated with switched-capacitors. This results in providing a wide-range boost operation, allows flexibly design that required voltage gain only by properly selecting the turn ratio of the coupled-inductors. In addition, the size of the passive components of converters in [21]–[24] becomes comparably smaller than their competitors. By combining the KY model [25] with a conventional rectified step-down converter, a novel step-down/step-up DC converter is provided in the converter which can realize the continuous output current port with similar polarity to input and output. However, in this converter two switches are used. A new step-down/step-up converter that could eliminate existing deficiencies was presented in [26]. Continuous input/output current port and number of the components has been utilized in such a converter, but

relatively numerous diodes are employed which leads to more power losses and complicated circuit topology. A quadrature buck-boost converter with two power switches, with continuous input/output current and positive output polarity was presented in [27]. Of course, increasing the number of switches results in increasing complexity of the control circuit for the power MOSFETS. The buck-boost converter is highly used in photovoltaic applications. This study introduces a novel converter based on the conventional ZETA converter and the one in [20]. The proposed converter introduces a wide-range-gain buck-boost operation with the help of integration of a cell of switched-coupled-inductors within the conventional converter of [20]. Since the turn ratio of the coupled-inductors contributes in the voltage gain design, by appropriately choosing the turn ratio, one can reduce the components' sizes compared to the original circuits while benefiting from various buck-boost operations. A lower number of components accompanied with the smaller size of required components and the fewer components voltage and current stresses are the suggested converter's main advantages, which reduce its volume and cost of the implementation. The principles of operation and the properties of the presented converter are investigated in the following and the experimental tests are used to validate the claims.

## 2. PROPOSED CONVERTER

The most important points for DC-DC converters which are used in various applications can be mentioned as high

efficiency, low counterpart, low cost. The proposed converter plays a significant role in electric car, and both DC and AC microgrid applications shown in Fig. 2.

Fig. 3 represents the circuit configuration of the presented converter. As seen in this figure, the internal cell of the switched-capacitors of the converter of [20] is reconfigured using the coupled-inductors.

In fact, the inductor  $L_2$  of the converter

proposed in [20] is replaced by a set of three winding coupled-inductors. The new switched-coupled-inductor cell is inserted within the conventional ZETA converter in which employs a switch  $S_1$  two capacitors  $C_1$ ,  $C_2$  and two inductors  $L_1$  and  $L_2$ .

As seen in Fig. 3, the proposed converter is introduced in types I and II by reversing the dotted node of the winding  $N_1$ .

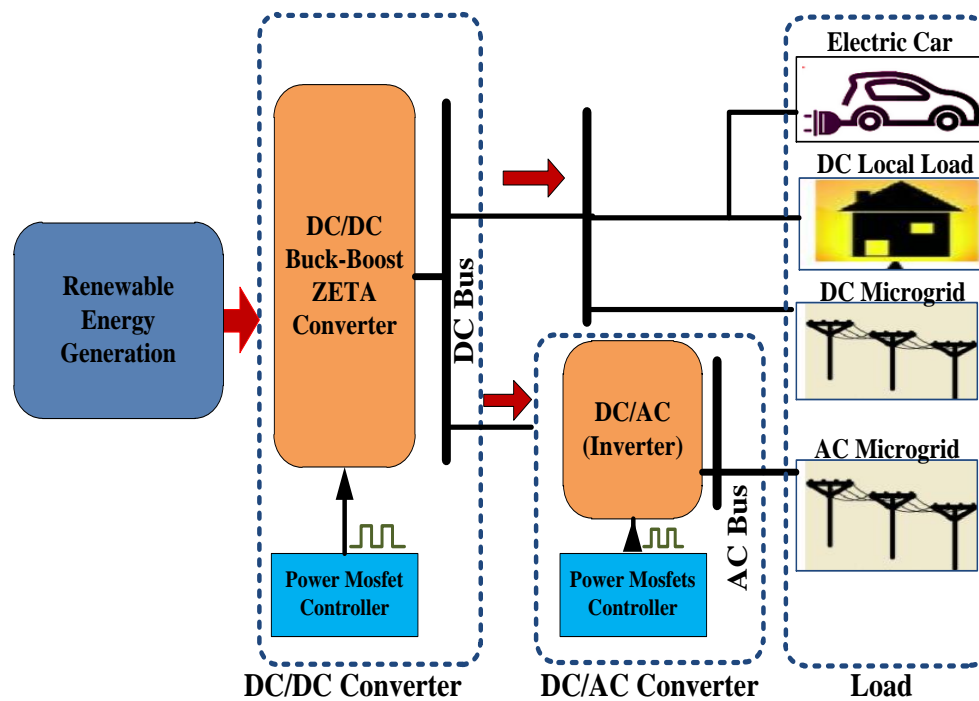


Fig. 2. DC/DC Converter applications.

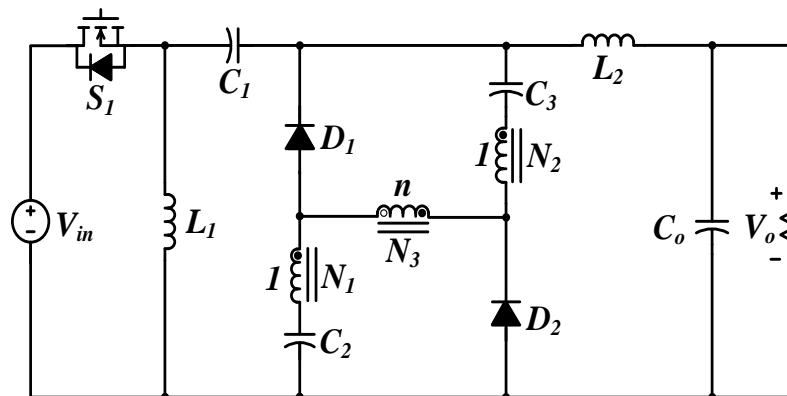


Fig. 3. Proposed wide-range-gain (WRG) ZETA converter.

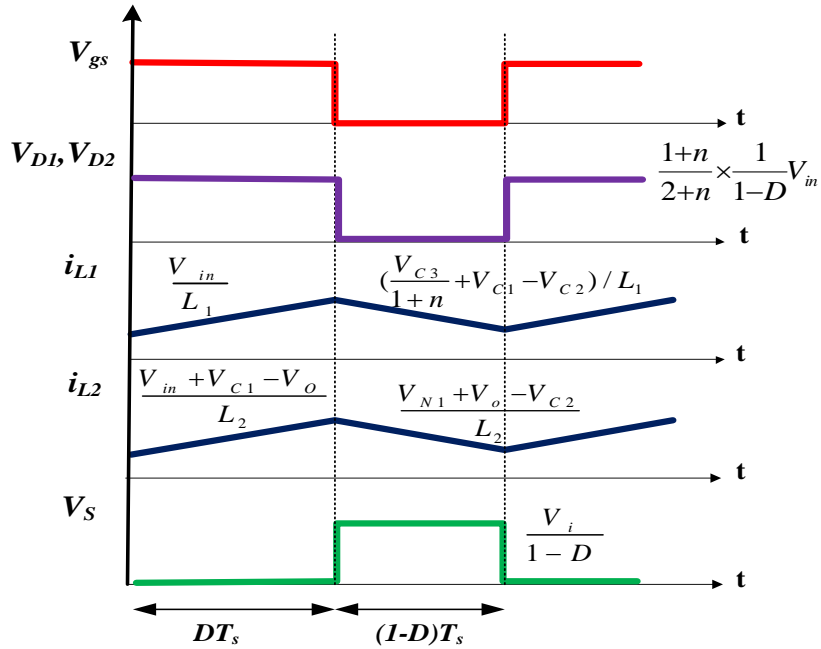


Fig. 4. Typical wave forms acting based on derived equations operating in proposed converter's CCM mode.

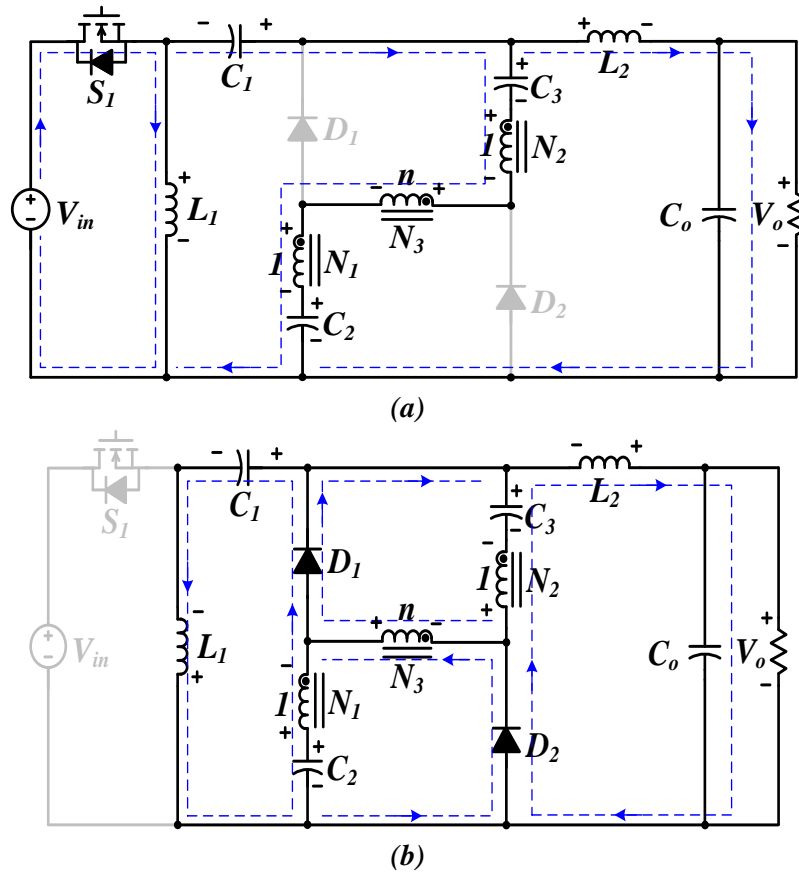


Fig. 5. Equivalent circuit of (a) mode I and (b) mode II of proposed WRG-ZETA converter.

Some of the charging and discharging states are vividly represented through time-domain characteristic waveforms in Fig 4.

## 2.1. Operation Principles

The proposed converter has two distinct mode of operation. Mode I is the On-state of the switch and mode II occurs when this switch turns OFF. With assuming type I of the presented converter, these two modes are analyzed in the following.

### 2.1.1. Mode I

In this operation mode, by turning on switch  $S_1$ , the diodes  $D_1$  and  $D_2$  are reversely biased and blocked their voltage, as presented in Fig. 5(a). The inductor  $L_1$  is charging by the input voltage source while the inductor  $L_2$  the same as the coupled-inductors and the capacitors  $C_2$  and  $C_3$  gain their energy from the input source and capacitor  $C_1$  in series. Also, the load is supplied by the input voltage source and the capacitor  $C_1$ . The average voltage equations of this mode are calculated from its equivalent circuit scheme, presented in Fig. 5(a), as,

$$V_{L1} = V_{in} \quad (1)$$

$$V_{L2} = V_{in} + V_{C1} - V_o \quad (2)$$

$$V_{N1} = \frac{V_{in} + V_{C1} - V_{C2} - V_{C3}}{(2+n)} \quad (3)$$

### 2.1.2. Mode II

By turning off the power MOSFET switch  $S_1$ , the stored energy of inductor  $L_1$  is discharged through the capacitor  $C_1$ . Simultaneously, the

energy kept in the coupled-inductors, the capacitor  $C_2$  and  $C_3$  and the inductor  $L_2$  supply the output load through the diodes  $D_1$  and  $D_2$  in this manner. Fig. 5(b) represents the equivalent circuit of this mode where the output current continuously flows through the load during both modes of the operation. The voltage equations of the suggested converter in this mode are given as,

$$V_{L1} = \frac{V_{C3}}{1+n} + V_{C1} - V_{C2} \quad (4)$$

$$V_{L2} = V_{N1} + V_o - V_{C2} \quad (5)$$

$$V_{N1} = \frac{V_{C3}}{1+n} \quad (6)$$

Employing the volt-second balance on the voltages across the inductors and the windings of the coupled-inductor, given in (1)-(6), the voltages of the capacitors  $C_1$ ,  $C_2$  and  $C_3$ , and the output voltage are calculated as,

$$V_{C1} = V_o \quad (7)$$

$$V_{C2} = V_{C3} = \frac{V_o}{2} \quad (8)$$

$$V_o = \frac{2(1+n)}{2+n} \times \frac{D}{1-D} V_{in} \quad (9)$$

Therefore, the voltage gain of the type I of the proposed converter is,

$$G^{TypeI} = \frac{V_o}{V_{in}} = \frac{2(1+n)}{2+n} \times \frac{D}{1-D} \quad (10)$$

For type II of the proposed converter, one can conclude that since the dotted node of the winding  $N_3$  is reversed, simply by changing

the turn ratio sign within (1)-(10), the voltage gain of the type II of the proposed converter can be obtained.

As seen from (10), the turn ratio of the coupled-inductor contributes in the voltage gain of the suggested converter in addition to the duty cycle of the switch  $S_1$ . This increases the voltage gain degree of freedom to design

various gain operations for any required application. To represent and compare the voltage gain of the suggested converter among other conventional competitors, it is plotted in Fig. 6 for various turn ratios. It is observed that the voltage gain of the provided converter can be designed such that provides a wide-range buck-boost operation.

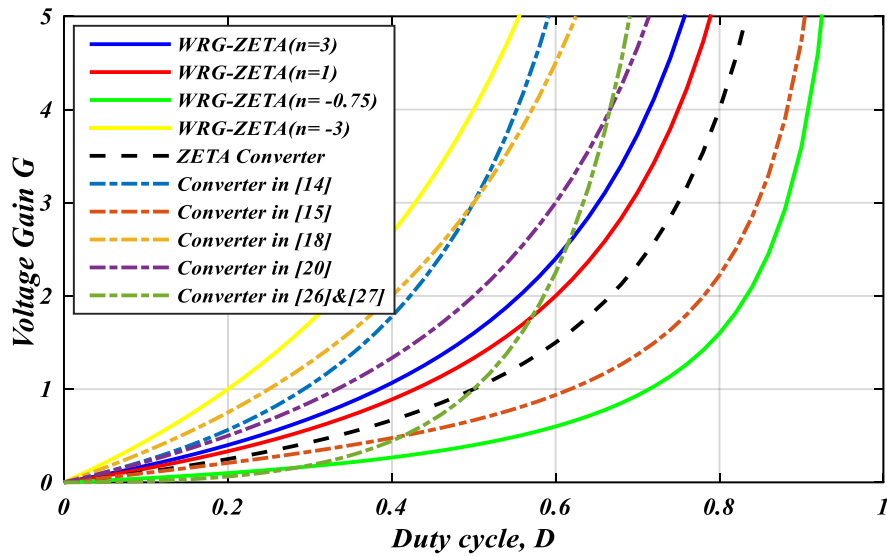


Fig. 6. Voltage gain versus duty cycle.

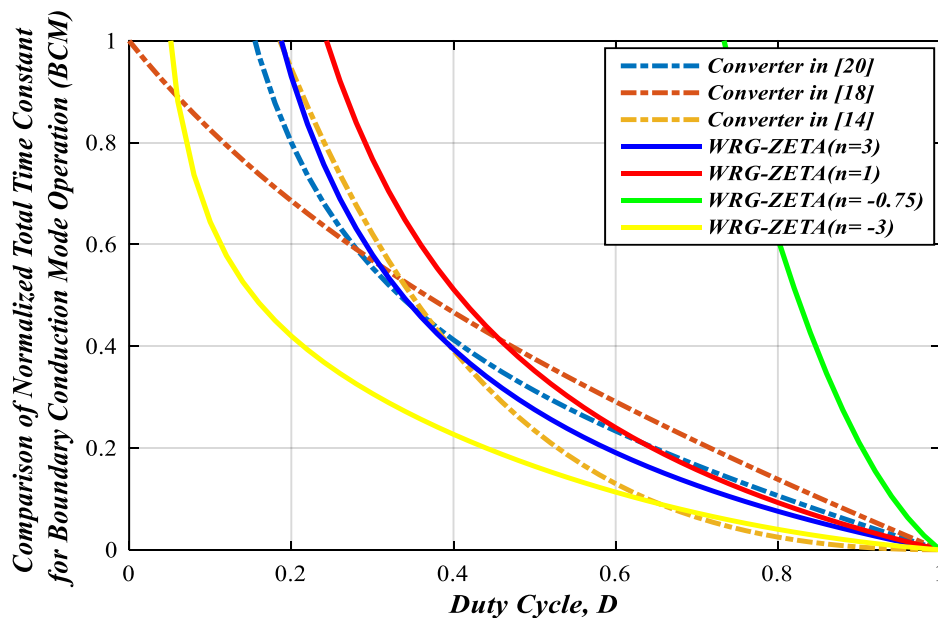


Fig. 7. Comparison of normalized total time constant for boundary conduction mode operation.

## 2.2. Components Design and Criteria

In order to measure and compare the properties of any power converter, it is essential for the component parameters to be designed based on the same criteria. The components of the suggested converter are designed in this section and compared with other conventional converters.

### 2.2.1. Inductive Component

The coupled and discrete inductors must be designed such that the continuous conduction mode (CCM) of operation is guaranteed for the proposed converter. With considering this requirement, the CCM condition is calculated in terms of the corresponding circuit provided in Fig. 5(a) for the inductors  $L_1$  and  $L_2$ , and the magnetizing inductance of coupled-windings as below.

$$\begin{cases} L_1 \geq \frac{((1-D)(2 \pm n))^2}{8D(1 \pm n)^2} \times \frac{R_o}{f_s} \\ L_2 \geq \frac{(1-D)(2 \pm n)}{4(1 \pm n)} \times \frac{R_o}{f_s} \end{cases} \quad (11)$$

$$L_m \geq \frac{(1-D)^2}{8(1 \pm n)^2} \times \frac{R_o}{f_s} \quad (12)$$

where,  $f_s$  is the switching frequency and  $R_o$  is the load resistance.

The total inductance of the coupled-windings of the proposed converter is then obtained as,

$$L_c^{tot} = (2+n^2)L_m \quad (13)$$

By using (13), the CCM condition for the coupled-windings is rewritten as,

$$\begin{aligned} L_c^{tot} &= (2+n^2)L_m \geq \frac{(1-D)^2}{8(1 \pm n)^2} (2+n^2) \times \frac{R_o}{f_s} \rightarrow \\ L_c^{tot} &\geq \frac{(1-D)^2}{8(1 \pm n)^2} (2+n^2) \times \frac{R_o}{f_s} \end{aligned} \quad (14)$$

In order to measure the total inductive component required to guarantee the CCM operation of the suggested converter, one can write the normalized total time constant of the inductive components with using (11) and (14) as,

$$\begin{aligned} \tau_{tot} &\geq \frac{(1-D)^2(2 \pm n)^2 + 2(1-D)D(1 \pm n)(2 \pm n)}{8D(1 \pm n)^2} \\ &+ \frac{D(1-D)^2(2+n^2)}{8D(1 \pm n)^2} \end{aligned} \quad (15)$$

where,

$$\begin{aligned} \tau_{tot} &= \tau_1 + \tau_2 + \tau_c^{tot} \\ &= \frac{L_1 f_s}{R_o} + \frac{L_2 f_s}{R_o} + \frac{L_c^{tot} f_s}{R_o} \end{aligned} \quad (16)$$

The normalized total time constant of the inductive components is also calculated for the converters of [14],[18] and [20] in Fig. 7. Evidently, the area above each curve of Fig. 7 is the CCM area and below that is the DCM area. In other words, if the inductances are designed such that guarantee the normalized total time constant to be higher than the corresponding curve, one can say that the converter operates in CCM. As seen from Fig. 7, the extra freedom level to design the voltage gain of the proposed converter allows to desirably change the CCM area compared with [14],[18] and [20].

### 2.2.2. Capacitive Components

The total capacitance of capacitors required for a power converter is one of the major parameters in measuring its advantages over the conventional ones. Therefore, the capacitances are designed with considering the maximum tolerable voltage ripple for the capacitors, which is defined by  $\alpha$ -time of their voltage. Consequently, assuming that the converter operates in mode I, one can write,

$$C = \frac{DI_c}{\alpha V_c f_s} \quad (17)$$

By using the (17) and regarding the equivalent circuit shown in Fig. 5(a), one can calculate,

$$C_1 = \left| \frac{2D(1 \pm n)}{(2 \pm n)} \right| \times \frac{1}{\alpha R_o f_s} \quad (18)$$

$$C_2 = C_3 = \left| \frac{\pm 2nD}{(2 \pm n)} \right| \times \frac{1}{\alpha R_o f_s} \quad (19)$$

The sum of the capacitances of  $C_1$ - $C_4$  is calculated and plotted for the proposed converter and the relevant converters are shown in Fig. 8. It is observed that the proposed converter voltage gain can be designed such that the required total capacitance becomes lower than of [20] and [18].

### 2.2.3. Electrical Stress on Semiconductor Components

The current and voltage stresses of the diodes and switches of a power converter contribute in its power loss and final cost of implementation. Therefore, these stresses must be evaluated. As an illustrative parameter, one can use the switching device power, i.e.  $SDP$ , as a measure for the converter cost and the power loss as already mentioned in [28]. The overall average switching device power ( $SDP_{avg}$ ) is calculated as,

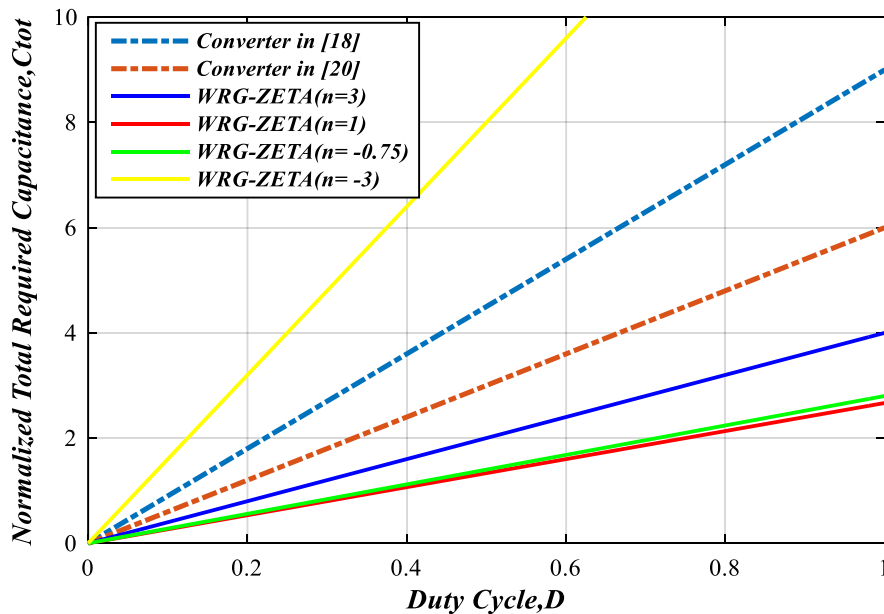


Fig. 8. Comparison of normalized total required capacitance.

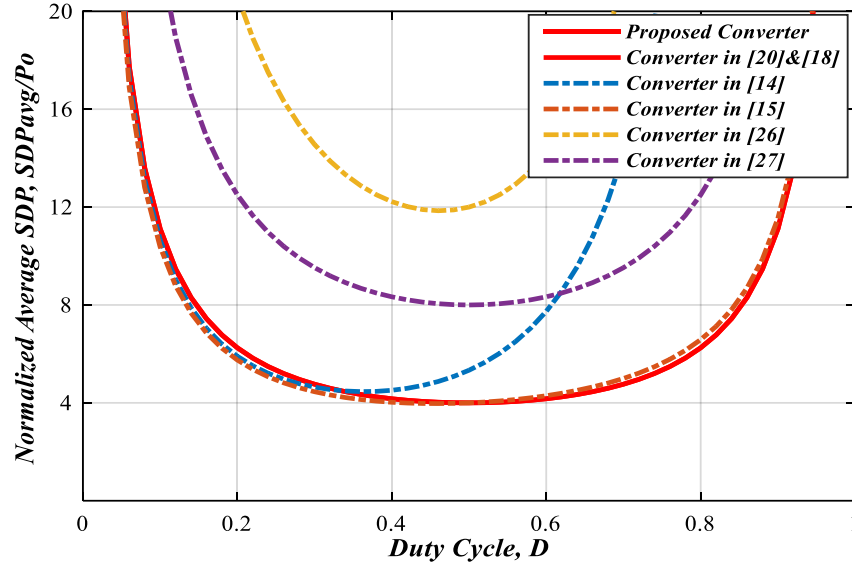


Fig. 9. Comparison of normalized total average switching device power ( $SDP_{avg}$ ).

$$SDP_{avg} = \sum_{i=1}^n V_{pk\_i} I_{avg\_i} \quad (20)$$

where,  $V_{pk\_i}$  and  $I_{avg\_i}$  are the peak voltage and average current of a switching period/duration of  $i^{\text{th}}$  semiconductor employed in a power converter. The peak voltage and the average current of the diodes and the switch of the proposed converter are calculated as,

$$\begin{cases} V_{pk}^{D_1} = V_{pk}^{D_2} = \frac{V_o}{2D} \\ V_{pk}^{S_1} = \frac{1}{1-D} V_{in} \end{cases} \quad (21)$$

$$\begin{cases} I_{avg}^{D_1} = I_{avg}^{D_2} = I_o \\ I_{avg}^{S_1} = I_{in} \end{cases} \quad (22)$$

From (21) and (22), one can calculate the total average  $SDP$  as,

$$SDP_{avg} = \left( \frac{1}{D(1-D)} \right) P_o \quad (23)$$

in which,  $P_o$  is the output power.

Fig. 9 represents the total average  $SDPs$  of the various converters. It is observed that the suggested converter offers lower  $SDP$  than the other competitors for  $D \geq 0.5$ , which directly translates to the lower power loss and cost of semiconductors. It is worth noting that the turn ratio of the coupled-inductors of the proposed converter does not contribute in the  $SDP_{avg}$ . This means that even with a wide-range-gain operation, the voltage and current stresses of the semiconductors of the presented converter is the same as those of their origin.

Finally, in order to compare the number of components and the properties of the proposed converter with other converters, Table 1 is presented.

#### 2.2.4. Voltage Stress of the Switch

In this converter, voltage stress on power MOSFET switch can be achieved as follows:

$$V_s = \frac{V_i}{1-D} \quad (24)$$

**Table 1. Comparison of Proposed Converter Among Recently Proposed Competitors.**

Parameter	Proposed Converter	Converter in [20]	Converter in [27]	Converter in [26]	Converter in [18]	Converter in [15]	Converter in [14]
No. of Switches	1	1	2	1	1	1	1
No. of Diodes	2	2	2	5	3	3	3
No. of Caps.	4	4	3	3	5	2	2
No. of Magnetic Cores	3	3	3	3	3	2	2
Number of elements	<b>10</b>	<b>10</b>	<b>10</b>	<b>12</b>	<b>12</b>	<b>8</b>	<b>8</b>
Voltage stress on switches ( $V_s/V_{in}$ )	$\frac{1}{1-D}$	$\frac{1}{1-D}$	$\frac{1}{(1-D)^2}$	$\frac{1}{(1-D)^2}$	$\frac{1}{1-D}$	$\frac{1}{1-D}$	$\frac{1}{(1-D)^2}$
Voltage stress on diodes ( $V_D/V_{in}$ )	$\frac{1+n}{2+n} \times \frac{1}{1-D}$	$\frac{1}{1-D}$	$\frac{1}{1-D}$	$\frac{1}{(1-D)^2}$	$\frac{1}{1-D}$	$\frac{1}{1-D^2}$	$\frac{1-D}{D}$
	$\frac{1+n}{2+n} \times \frac{1}{1-D}$	$\frac{1}{1-D}$	$\frac{D}{(1-D)^2}$	$\frac{1}{(1-D)^2}$	$\frac{1}{1-D}$	$\frac{D}{1-D^2}$	$\frac{1}{(1-D)^2}$
				$\frac{1}{(1-D)^2}$	$\frac{1}{1-D}$	$\frac{D}{1-D^2}$	$\frac{1}{(1-D)^2}$
Voltage stress on capacitor ( $V_C/V_{in}$ )	$\frac{2(1+n)}{2+n} \times \frac{D}{1-D}$	$\frac{2D}{1-D}$	$\frac{1}{1-D}$	$\frac{1}{1-D}$	$\frac{2D}{1-D}$	$\frac{D^2}{1-D^2}$	$\frac{D}{1-D}$
	$\frac{(1+n)}{2+n} \times \frac{D}{1-D}$	$\frac{D}{1-D}$	$\frac{1}{(1-D)^2}$	$\frac{1}{(1-D)^2}$	$\frac{D}{1-D}$	$\frac{D}{1-D^2}$	$\frac{D(2-D)}{(1-D)^2}$
	$\frac{(1+n)}{2+n} \times \frac{D}{1-D}$	$\frac{D}{1-D}$			$\frac{2D}{1-D}$	$\frac{D}{1-D^2}$	$\frac{D(2-D)}{(1-D)^2}$
Voltage Gain	$\frac{2(1+n)}{2+n} \times \frac{D}{1-D}$	$\frac{2D}{1-D}$	$\left(\frac{D}{1-D}\right)^2$	$\left(\frac{D}{1-D}\right)^2$	$\frac{3D}{1-D}$	$\frac{D}{1-D^2}$	$\frac{D(2-D)}{(1-D)^2}$
Norm. SDP <sub>avg</sub>	$\left(\frac{1}{D(1-D)}\right)$	$\left(\frac{1}{D(1-D)}\right)$	$\left(\frac{2-2D}{D(1-D)^2}\right)$	$\left(\frac{6D^2-8D+4}{D(1-D)^2}\right)$	$\left(\frac{1}{D(1-D)}\right)$	$\left(\frac{1+3D^2-2D^3}{D-D^3}\right)$	$\left(\frac{4D^2-4D+2}{D(1-D)^2(2-D)}\right)$

In Fig.10, the comparison between the normalized voltage stress across power switch of the presented converter and other types of similar converters is depicted. As seen in the suggested converter, the normalized voltage stress of the power MOSFET switch is less than in [14], [15], [26] and [27]. Table 1 presents the voltage stress across power switch other competitors.

### 3. EXPERIMENTAL VALIDATION

The suggested converter operation is evaluated in this section by a set of experimental tests on a prototype setup built with the parameters and components given in Table 2. For the boost mode operation, the proposed converter operates to raise the input

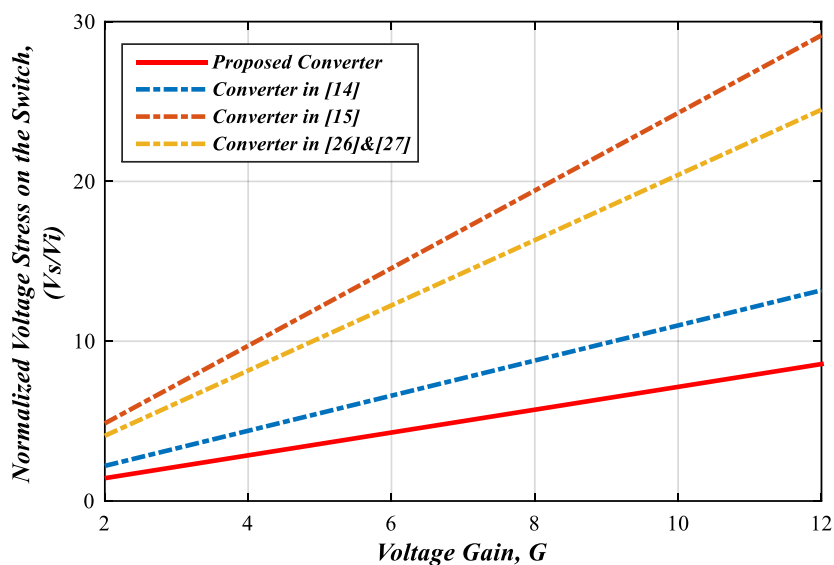


Fig. 10. Comparison of normalized switch voltage stress.

Table 2. Experimental Parameters and Conditions.

Parameters and Components	Values and Part Numbers
Input Voltage, $V_{in}$	$36V_{dc} \sim 120V_{dc}$
Output Voltage, $V_o$	$100V_{dc}$
Output Power, $P_o$	200W
Switching Frequency, $f_s$	40kHz
Discrete Inductors, $L_1$ & $L_2$	$300\mu H$ & $1mH$
Magnetizing Inductor, $L_m$ ( $N_1:N_2:N_3$ )	$200\mu H$ (12:6:12)
Capacitors, $C_1=C_2=C_3=C_o$	$22\mu F$
Diode, $D_1$ & $D_2$	MUR860
Switch, $S_1$	IRFP460A

voltage of  $36V_{dc}$  to  $100V_{dc}$  at the output side while the buck mode operation, it decreases the input voltage of  $120V_{dc}$  to  $100V_{dc}$  to feed a 200W output load.

By using a set of three coupled-windings on an EE ferrite magnetic core with the turn ratio of  $n = 0.5$ , as given in Table 2, the wide-

range-gain operation of the suggested converter is investigated and approved in the following. From (10), one can calculate the duty cycle for the boost mode of type I as  $D = 0.7$  and that of type II as  $D = 0.8$ . Also, for the buck operation, the duty cycles are  $D = 0.41$  and  $D = 0.56$  for the type I and type II of

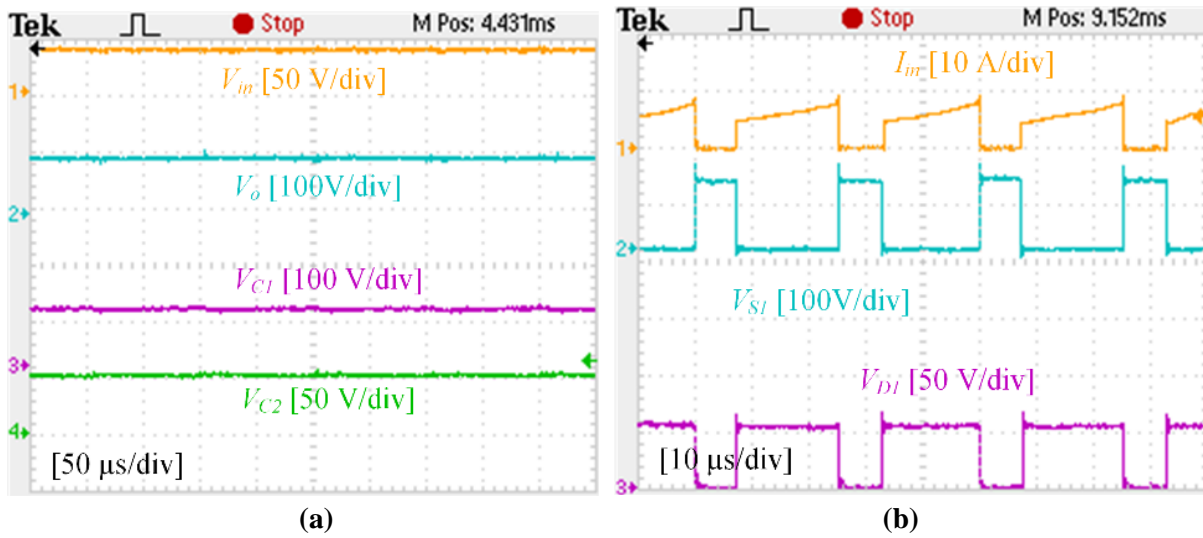


**Fig. 11.** Waveforms of (a) input, output, capacitors C1 and C2 voltages, and (b) input current and voltages across switch S1 and diode D1 measured from the boost mode of type I of proposed converter.

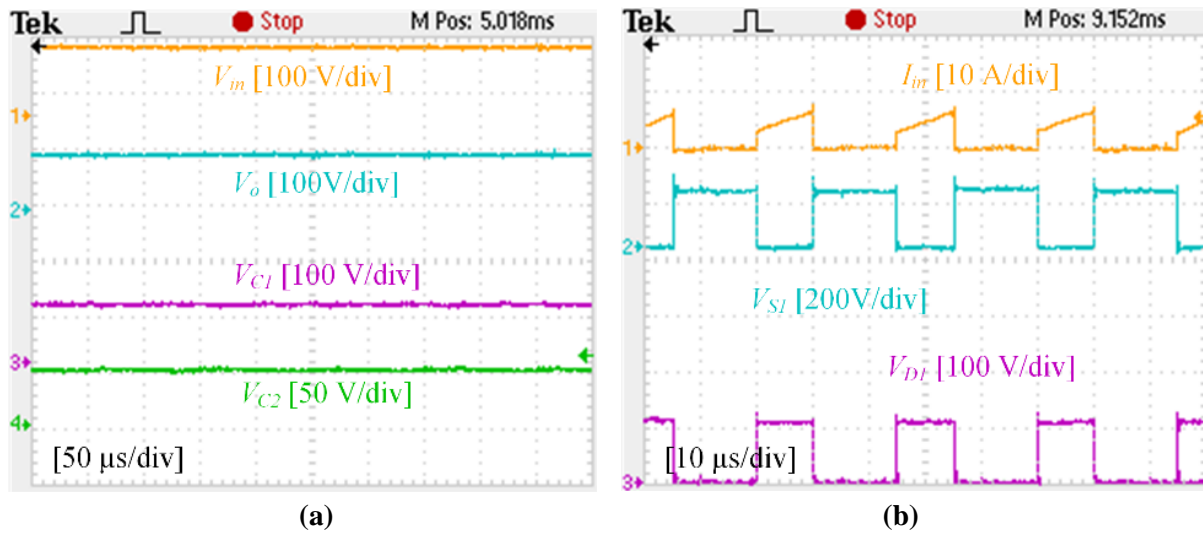


**Fig. 12.** Waveforms of (a) input, output, capacitors C1 and C2 voltages, and (b) input current and voltages across switch S1 and diode D1 measured from the buck mode of type I of proposed converter

the proposed converter, respectively. Since, the operation principles of the suggested converter are the same for the inductances of  $L_1$ ,  $L_2$  and the magnetizing inductance of  $L_m$  are selected higher than the limits of (11) and (12) such that the CCM operation is guaranteed.

In addition, the capacitors are designed using (18) and (19) with assuming that their voltage ripples are restricted to 10% of their peak voltage.

The output and input voltages along with the voltages of the capacitors C1 and C2 are measured when the type I of the suggested

converter operates in its boost mode which is shown in Fig. 11(a). The voltages across the switch S1, the diode D1 and the input current is also shown in Fig. 11(b) for this mode of operation. As seen in these figures, the proposed converter successfully increases the input voltage to the desired output voltage and the semiconductors operation are fully adapted with the claims in section 2. The voltages across the switch S1 and the diode D1 are measured as 120Vdc and 70Vdc, respectively, which are the same as the values calculated from (21). For the buck mode of the proposed converter, the same waveforms are measured and shown in Figs. 12. As obviously seen from Fig. 12(a), the suggested converter decreases the input voltage of 120Vdc to 100Vdc while its operation principles are validated by the measured waveforms of the voltages across the switch S1 and diode D1, as provided in Fig. 12(b).

Finally, from the test results, it is concluded that the proposed converter operation is completely validated and the principles of operation and the properties claimed in previous sections are all confirmed.

#### 4. CONCLUSION

This paper introduces a new modified ZETA converter, which benefits from a set of switched-coupled-inductors. The proposed converter presents a wide-range-gain buck-boost operation with properly selecting the turn ratio of its coupled-inductors. The size of the required passive components along with the current and voltage stresses of the proposed converter are comparably less than the previous successful competitors. Therefore, the proposed converter is an

attractive converter for the applications, in which the output voltage should be regulated from an unregulated variable input voltage source, such as the storage batteries, LED drivers and fuel cells. The theoretical claims and features are derived and investigated. Then, the principles of operation of the proposed converter are validated through a set of experimental tests on a prototype built in the laboratory.

#### REFERENCES

- [1] F. Blaabjerg, R. Teodorescu, and M. Liserre, "Power converters and control of renewable energy systems," in Proc. Int. Conf. Perform. Eng, pp. 2–20, Oct. 2004.
- [2] F. Blaabjerg, Z. Chen, and S. B. Kjaer, "Power Electronics as Efficient Interface in Dispersed Power Generation Systems," IEEE Trans. Power Electron, vol. 19, no. 5, pp. 1184–1194, Sep. 2004.
- [3] M. Taghvaei, M. Radzi, S. Moosavain, H. Hizam, M. H. Marhaban, "A current and future study on non-isolated DC–DC converters for photovoltaic applications." Renewable and Sustainable Energy Review, vol.17, pp. 216–27, Jun. 2013.
- [4] T. V. Jensen and P. Pinson, "RE-Europe, a large-scale dataset for modeling a highly renewable European electricity system," Scientific Data, vol. 4, pp. 170175, 2017.
- [5] A. Tahri, H. E. Fadil, F. Z. Belhaj, K. Gaouzi, A. Rachid, F. Giri, F. Z. Chaoui, "Management of fuel cell power and supercapacitor state-of-

- charge for electric vehicles,” *Int. J. Electric Power Systems Research*, vol. 160, pp. 89-98, July. 2018.
- [6] R. Reshma Gopi, S. Sreejith, “Converter topologies in photovoltaic applications – A review,” *Int. J. Renewable and Sustainable Energy Reviews*, vol. 94, pp. 1-14, Oct. 2018.
- [7] R. W. Erickson, “*Fundamentals of Power Electronics*”, 2nd ed. Norwell, MA: Kluwer, 2001.
- [8] D.C. Martins, F. de Souza Campos, I. Barbi, “Zeta Converter with High Power Factor Operating in Continuous Conduction Mode,” *Proceedings of Intelec'96 - International Telecommunications Energy Conference*, pp. 107-113, Oct. 1996.
- [9] A. Ioinovici, “Switched-capacitor power electronics circuits,” *IEEE Circuits Syst. Mag.*, vol. 1, no. 3, pp. 37-42, 2001.
- [10] H. S. H. Chung, A. Ioinovici, and W. L. Cheung, “Generalized structure of bi-directional switched-capacitor DC/DC converters,” *IEEE Trans. Circuits Syst. I Fundam. Theory Appl.*, vol. 50, no. 6, pp. 743-754, 2003.
- [11] L. S. Yang, T. J. Liang, and J. F. Chen, “Transformerless DC-DC converters with high step-up voltage gain,” *IEEE Trans. Ind. Electron*, vol. 56, no. 8, pp. 3144-3152, 2009.
- [12] S. Iqbal, “A hybrid symmetrical voltage multiplier,” *IEEE Trans. Power Electron*, vol. 29, no. 1, pp. 6-12, 2014.
- [13] M. Prudente, L. L. Pfitscher, G. Emmendoerfer, E. F. Romaneli, and R. Gules, “Voltage Multiplier Cells Applied to Non-Isolated DC-DC Converters,” *IEEE Trans. Power Electron*, vol. 23, no. 2, pp. 871-887, Mar. 2008.
- [14] S. A. Gorji, A. Mostaan, H. T. My, and M. Ektesabi, “Non-isolated buck-boost dc-dc converter with quadratic voltage gain ratio,” *IET Power Electron*, vol. 12, no. 6, pp. 1425-1433, 2019.
- [15] J. Li and J. Liu, “A Novel Buck-Boost Converter with Low Electric Stress on Components,” *IEEE Trans. Ind. Electron*, vol. 66, no. 4, pp. 2703-2713, 2019.
- [16] S. Miao, F. Wang, and X. Ma, “A New Transformerless Buck-Boost Converter with Positive Output Voltage,” *IEEE Trans. Ind. Electron*, vol. 63, no. 5, pp. 2965-2975, 2016.
- [17] S. Ding and F. Wang, “A New Negative Output Buck-Boost Converter with Wide Conversion Ratio,” *IEEE Trans. Ind. Electron*, vol. 64, no. 12, pp. 9322-9333, 2017.
- [18] M. R. Banaei and H. A. F. Bonab, “A Novel Structure for Single-Switch Nonisolated Transformerless Buck-Boost DC-DC Converter,” *IEEE Trans. Ind. Electron*, vol. 64, no. 1, pp. 198-205, 2017.
- [19] M. R. Banaei and S. G. Sani, “Analysis and Implementation of a New SEPIC-Based Single-Switch Buck-Boost DC-DC Converter with Continuous Input Current,” *IEEE Trans. Power Electron*, vol. 33, no. 12, pp. 10317-10325, 2018.
- [20] M. R. Banaei and H. A. F. Bonab, “A High Efficiency Nonisolated Buck-Boost Converter Based on ZETA Converter,” *IEEE Trans. Ind. Electron*, vol. 67, no. 3, pp. 1991-1998, 2020.

- [21] S. Sharifi and M. Monfared, "Series and Tapped Switched-Coupled-Inductors Impedance Networks," *IEEE Trans. Ind. Electron*, vol. 65, no. 12, pp. 9498–9508, Dec. 2018.
- [22] S. Sharifi, F. Jahani, and M. Monfared, "Direct Single-Phase AC–AC Converters Based on Series Impedance Networks," *IEEE Trans. Power Electron*, vol. 33, no. 12, pp. 10380–10389, Dec. 2018.
- [23] S. Sharifi and M. Monfared, "Modified Series and Tapped Switched-Coupled-Inductors Quasi-Z-Source Networks," *IEEE Trans. Ind. Electron*, vol. 66, no. 8, pp. 5970–5978, Aug. 2019.
- [24] S. Sharifi, Y. Chulaee, H. Abootorabi, and M. Monfared, "Generalized Three-Winding Switched-Coupled-Inductor Impedance Networks with Highly Flexible Gain," *IEEE Trans. Ind. Electron.*, pp. 1–1, 2020.
- [25] K. I. Hwu and T. J. Peng, "A Novel Buck–Boost Converter Combining KY and Buck Converters," *IEEE Trans. Power Electron*, vol. 27, no. 5, pp. 2236–2241, May. 2012.
- [26] N. Zhang, G. Zhang, K. W. See, and B. Zhang, "A Single-Switch Quadratic Buck-Boost Converter with Continuous Input Port Current," *IEEE Trans. Power Electron*, vol. 33, no. 5, pp. 4157–4166, June. 2018.
- [27] N. A. Sarikhani, B. Allahverdinejad, M. Hamzeh, E. Afjei, "A Continuous Input and Output Current Quadratic Buck-Boost Converter with Positive Output Voltage for Photovoltaic Applications." *Solar Energy*, vol. 188, pp. 19–27, Aug. 2019.
- [28] N. M. Shen, A. Joseph, J. Wang, F. Z. Peng, and D. J. Adams, "Comparison of Traditional Inverters and Z-Source Inverter for Fuel Cell Vehicles," *IEEE Trans. Power Electron*, vol. 33, no. 4, pp. 1453–1463, Jul. 2007.